Linearly and curvilinearly tapered cylindrical- dielectric-rod antennas

ANDO, Takashi / NAKANO, Hisamatsu / YAMAUCHI, Junji / NUMATA, Satoshi / OHBA, Isao

(出版者 / Publisher)
IEEE

(雑誌名 / Journal or Publication Title)
IEEE Transactions on Antennas and Propagation / IEEE Transactions on Antennas and Propagation

(号 / Number)
9

(開始ページ / Start Page)
2827

(終了ページ / End Page)
2833

(発行年 / Year)
2005-09

Linearly and Curvilinearly Tapered Cylindrical-Dielectric-Rod Antennas

Takashi Ando, *Member, IEEE*, Isao Ohba, Satoshi Numata, Junji Yamauchi, *Member, IEEE*, and Hisamatsu Nakano, *Fellow, IEEE*

***Abstract*—The body-of-revolution finite-difference time-domain (BOR-FDTD) method is applied to the analysis of a tapered cylindrical-dielectric-rod fed by a metallic waveguide with a launching horn. Before evaluating the wave propagating along the tapered rod, we design the launching horn to efficiently excite the fundamental guided-mode of a uniform rod. After confirming the effectiveness of the launching horn, guided-mode conversion properties are evaluated in linearly and curvilinearly tapered rods. As a result, the guided mode excited at the feed end is smoothly converted into that at the free end in a curvilinearly tapered rod. It is numerically revealed that the smooth guided-mode conversion leads to the expansion of the equiphase field region in a terminal aperture with a subsequent increase in the gain. The calculated radiation patterns are in good agreement with experimental data.**

***Index Terms*—Antenna theory, dielectric antennas, dielectric waveguides, endfire antennas, finite-difference time-domain (FDTD) methods.**

I. Introduction

MANY researchers [1]–[11] have been studying the radiation mechanism and characteristic of a dielectric rod antenna at microwave and millimeter-wave frequencies. Two practical antenna structures, which have mainly been investigated, are a uniform rod and a tapered rod fed by a metallic waveguide.

The radiation mechanism of a uniform rod [2]–[4] was interpreted by Zucker's discontinuity-radiation concept [1]. To demonstrate the concept, we have recently succeeded in quantitatively evaluating the guided wave propagating along the uniform rod and the unguided wave radiating near the feed end [12]. The gain variation with rod length has also been explained in terms of the expansion of the equiphase field region in a terminal aperture [13], where the secondary source field is composed of the guided and unguided waves. It is emphasized that the exact information on the behavior of the waves propagating along the rod is important to evaluate the radiation characteristics.

It is generally known that the gradual taper of a dielectric rod leads to an increase in the gain [5]–[8]. So far, the directivity of a tapered rod has been estimated using traditional design guidelines [9]. Zucker [10] presented a design principle for a maximum-gain antenna, in which a tapered rod is regarded as an endfire array of discrete elements. James [11] described a semi-empirical approach to the selection of an optimum taper profile, in which a tapered rod is regarded as a series of noninteracting planar radiating apertures. It should be noted, however, that the design procedure of a taper profile has not been established, since the previous studies did not give information on the change in the guided wave in a tapered rod. This results in the fact that the attainable gain of a practical rod antenna may be limited to 20 dBi [9]–[11], although the traditional design guidelines predict the gain increase with an increase in rod length.

In this paper, we numerically analyze a tapered cylindrical-dielectric-rod fed by a metallic waveguide with a launching horn, and discuss the effect of the guided-mode conversion in the rod on the directivity. The waves propagating along linearly and curvilinearly tapered rods are evaluated using the body-of-revolution finite-difference time-domain (BOR-FDTD) method [14]–[16]. The use of the BOR technique enables us to efficiently calculate long cylindrical-dielectric-rods [17].

To evaluate the essential property of the guided wave in a tapered rod, we first eliminate the effect of the unguided wave radiated near the feed end. A launching horn is designed to efficiently excite the fundamental guided-mode of a uniform rod. It is demonstrated that the unguided wave is substantially reduced by the use of the launching horn.

Next, guided-mode conversion properties are evaluated in linearly and curvilinearly tapered rods. Calculations show that the fundamental guided-mode excited at the feed end is smoothly converted into that at the free end in a curvilinearly tapered rod. It is revealed that the smooth guided-mode conversion leads to the expansion of the equiphase field region in a terminal aperture with a subsequent increase in the gain. A gain of greater than 22 dBi is obtained for the curvilinearly tapered rod with a length of 20λ. The gain characteristics obtained from the FDTD analysis are compared with those from the traditional design guideline [10]. Experiments were performed to confirm the directivity calculations.

II. Configuration and Numerical Method

Fig. 1(a) shows the configuration of a cylindrical-dielectric-rod fed by a circular metallic waveguide. The rod with a relative permittivity of $\varepsilon_r = 2$ (Teflon) is assumed to be a lossless medium, and is composed of a uniform section (L_{uni}) and a tapered section (L_{tap}). The bore of the metallic waveguide, which is the same as the diameter of the uniform rod, is $2\rho_{\mathrm{feed}} = 17.475$ mm $(= 0.64\lambda)$ where λ (=27.3 mm) is the wavelength at a test frequency of $f = 11$ GHz. The metallic waveguide is excited with the TE_{11} mode, whose cutoff frequency is 10 GHz. The uniform rod operates as a single mode

Manuscript received January 20, 2004.

T. Ando is with Hitachi Research Laboratory, Hitachi, Ltd., Ibaraki 319-1292, Japan.

I. Ohba is with Toshiba Corporation, Tokyo 198-8710, Japan.

S. Numata is with Sony Corporation, Tokyo 140-0002, Japan.

J. Yamauchi and H. Nakano are with the Faculty of Engineering, Hosei University, Tokyo 184-8584, Japan (e-mail: j.yma@k.hosei.ac.jp).

Digital Object Identifier 10.1109/TAP.2005.854551

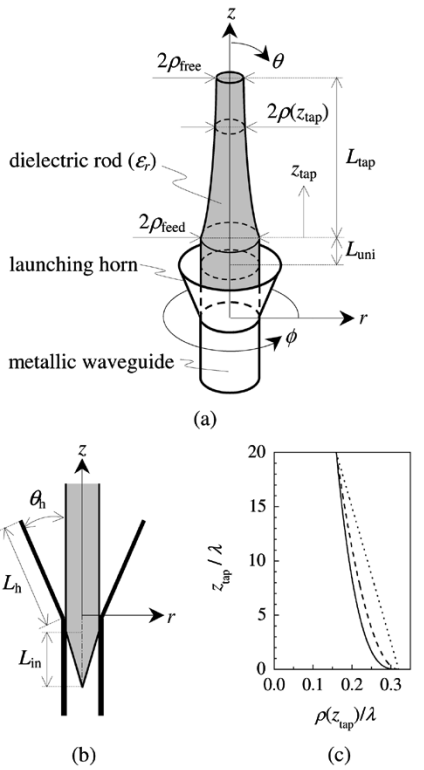

Fig. 1. Configuration of a tapered cylindrical-dielectric-rod antenna [$\varepsilon_r = 2$ (Teflon), $2\rho_{\rm feed} = 17.475$ mm ($= 0.64\lambda$), $2\rho_{\rm free} = \rho_{\rm feed}$, $\lambda = 27.3$ mm ($f = 11$ GHz)]. (a) Perspective view. (b) Feeding system. (c) Taper profiles for $L_{\rm tap} = 20\lambda$; linear ($n = 1$)..., curvilinear ($n = 2$)- - -, curvilinear ($n = 3$)—.

waveguide at the test frequency (The cutoff frequency of higher order modes [18] is 13 GHz).

To obtain smooth transition from the $\rm TE_{11}$ mode of the metallic waveguide to the $\rm HE_{11}$ mode of the uniform rod, we introduce the feeding system illustrated in Fig. 1(b). A portion of the uniform rod is tapered and inserted into the metallic waveguide. A launching horn is placed at the feed end. The performance of the feeding system will be discussed in Section III-A.

Typical taper profiles to be investigated are shown in Fig. 1(c), in which the diameter at the free end is taken to be $2\rho_{\rm free} = \rho_{\rm feed}$ and the overall length of the tapered section is fixed to be $L_{\rm tap} = 20\lambda$. The change in the radius of the tapered section, $\rho(z_{\rm tap})$, is expressed as

$$\rho(z_{\rm tap}) = \rho_{\rm feed} - (\rho_{\rm feed} - \rho_{\rm free}) \left(\frac{z_{\rm tap}}{L_{\rm tap}}\right)^{\frac{1}{n}} \qquad (1)$$

where $z_{\rm tap}$ is the axial distance of the tapered section [see Fig. 1(a)]. The rod of $n = 1$ is linearly tapered and that of $n > 1$ is curvilinearly tapered. For the curvilinear taper, the change in the radius near the feed end becomes large with an increase in n, while that near the free end becomes small. The guided-mode conversion properties and directivities will be evaluated in the linearly and curvilinearly tapered structures with $L_{\rm tap} = 10\lambda$ and 20λ in Section III-B.

The wave propagating along the rod is calculated by the BOR-FDTD method developed for the analysis of axially symmetric

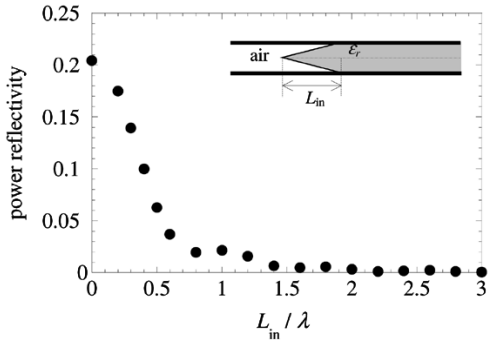

Fig. 2. Power reflectivity as a function of $L_{\rm in}$.

structures [14], [15]. By the use of the BOR technique, a circular interface is accurately described in the cylindrical coordinates based on Yee's mesh. Furthermore, the partial derivative with respect to ϕ can be performed analytically. Consequently, the original three-dimensional (r, ϕ, z) model is reduced to an equivalent two-dimensional (r, z) one. This leads to the fact that the wave propagating along a long rod can efficiently be analyzed. The grid widths are fixed to be $\Delta r = \rho_{\rm feed}/30$ and $\Delta z = \lambda/100$ throughout this analysis.

The boundary condition based on second-order Higdon's operator [15] is employed for absorbing outgoing waves at the computational edges. It should be noted that the free end of the rod is also terminated with the absorbing boundary condition. This enables us to evaluate the wave in a tapered rod dominated by a forward-traveling wave [12], [13], since the reflected wave generated at the free end is eliminated. We will confirm in Fig. 5 that the reflected wave does not significantly affect the gain characteristic.

The excitation scheme of a $+z$-propagating incident waveform [19] is used for a continuous wave simulation of the $\rm TE_{11}$ mode. The directivity is calculated from fields on a virtual closed surface regarded as a Huygens plane which encloses the antenna structure in the computational region [15], [16].

III. Results

A. Feeding System

To evaluate the essential property of the guided wave in a tapered rod, we eliminate the effect of the unguided wave radiated near the feed end. For this, the $\rm TE_{11}$ mode power excited in the metallic waveguide should mostly be converted into the $\rm HE_{11}$ mode power in the uniform rod. Hence, we discuss the feeding system composed of the launching horn and the uniform rod whose feed end is tapered and inserted into the metallic waveguide [see Fig. 1(b)]. Note that the directivity of the uniform rod ($L_{\rm tap} = 0$) is investigated for confirming the effectiveness of the feeding system. The method for configuring the parameters of the feeding system ($L_{\rm in}$, $L_{\rm h}$, and $\theta_{\rm h}$) is described in the following paragraphs.

The tapered rod inserted into the metallic waveguide is effective in the impedance matching between the air-filled and dielectric-filled regions in the waveguide. Fig. 2 plots the power reflectivity as a function of taper length $L_{\rm in}$. A reflectivity of less than 0.4%, which is equivalent to a return loss of 24 dB, is achieved for $L_{\rm in}$ greater than 2λ.

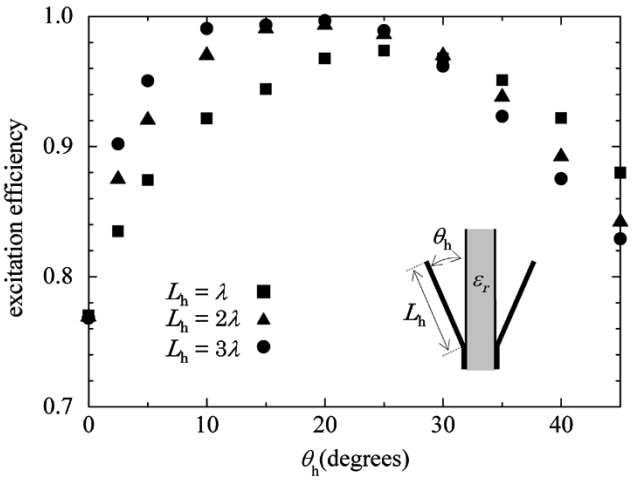

Fig. 3. Excitation efficiency of HE_{11} mode as a function of θ_h.

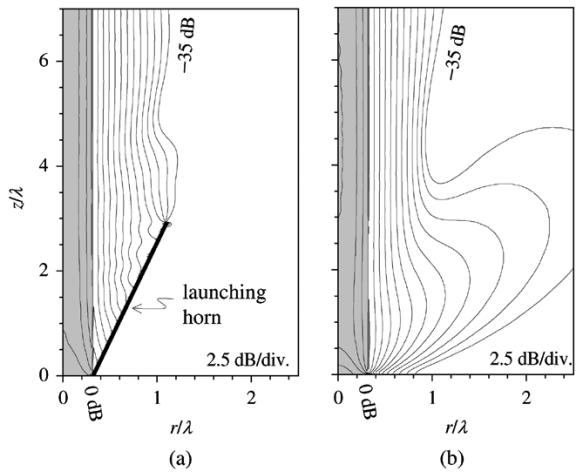

Fig. 4. Field distributions near feed end (half region). (a) With launching horn ($L_\mathrm{h} = 3\lambda, \theta_\mathrm{h} = 15°$). (b) Without launching horn.

The launching horn is effective in improving the excitation efficiency of the HE_{11} mode (the ratio of the HE_{11} mode power to the total radiation power). Fig. 3 shows the excitation efficiency against flare angle θ_h for three values of horn length L_h, in which the HE_{11} mode power is calculated using the overlap integral between the eigenmode field of the uniform rod and the numerically determined field. The data for $\theta_\mathrm{h} = 0$ corresponds to that for the rod without the launching horn. A value of greater than 98% is obtained over a range of $10° < \theta_\mathrm{h} < 25°$, when L_h is chosen to be 3λ.

Typical field distribution ($|\mathrm{E}_r|$ component) near the launching horn with $L_\mathrm{h} = 3\lambda$ and $\theta_\mathrm{h} = 15°$ is presented in Fig. 4(a). For comparison, the field for the rod without the launching horn is presented in Fig. 4(b). The shaded region represents the uniform rod. It is clearly observed that the unguided wave radiated near the feed end [Fig. 4(b)] is suppressed by using the launching horn [Fig. 4(a)].

From the above-mentioned results, the configuration parameters of the feeding system are fixed to be $L_\mathrm{in} = 2\lambda, L_\mathrm{h} = 3\lambda$, and $\theta_\mathrm{h} = 15°$ in the following investigations. As a result, the HE_{11} mode of the uniform rod is excited with an efficiency of 99% at a test frequency of $f = 11$ GHz. Further calculations

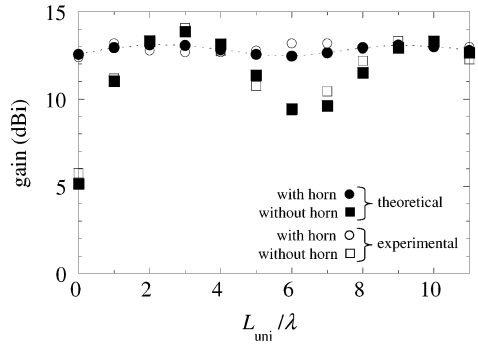

Fig. 5. Gain as a function of L_uni.

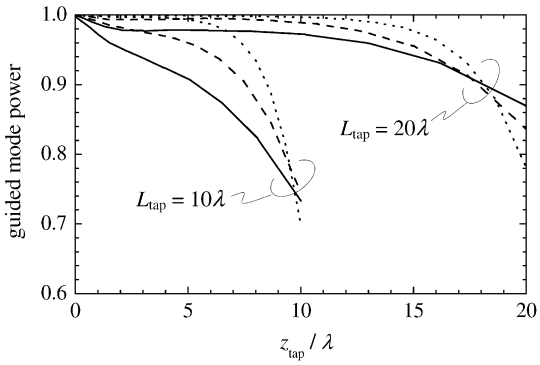

Fig. 6. Guided mode power as a function of z_tap; linear $(n = 1)\ldots$, curvilinear $(n = 2)- - -$, curvilinear $(n = 3)$—.

show that an excitation efficiency of greater than 99% is maintained over a frequency range of 11 to 12.7 GHz, while a return loss of greater than 15 dB is obtained.

We should recall that the directivity in the endfire direction is dominated by the source field in a terminal aperture [13] regarded as a secondary Huygens plane. Since the unguided wave is eliminated by the use of the launching horn, the directivity of the uniform rod must almost be characterized by the directivity generated from the HE_{11} mode field. The gain in the endfire direction, that is obtained from the HE_{11} mode field, is calculated to be 12.9 dBi.

Fig. 5 shows the gain against uniform-rod length L_uni. The data presented by solid circles are the calculated gain values for the rod with the launching horn, while the data presented by solid squares are those without the launching horn. When the launching horn is removed, the gain exhibits cyclical variation as a function of L_uni due to the phase interaction between the guided and unguided waves [13]. On the other hand, the gain for the rod with the launching horn varies only 12.8 ± 0.3 dBi with the change in L_uni. Fig. 5 also shows the measured gains for the uniform rod with the launching horn (open circles), together with those without the launching horn (open squares). It is demonstrated that the unguided wave is sufficiently suppressed by the use of the launching horn.

In practice, the uniform rod is terminated with air, so that the reflected wave is generated at the free end. To check the influence of the reflected wave on the gain, we also analyze the case for the open free end. Calculations of the rod with the launching horn show that the gain variation with L_uni is within 12.8 ± 0.35 dBi. Consequently, the experimental results plotted in Fig. 5

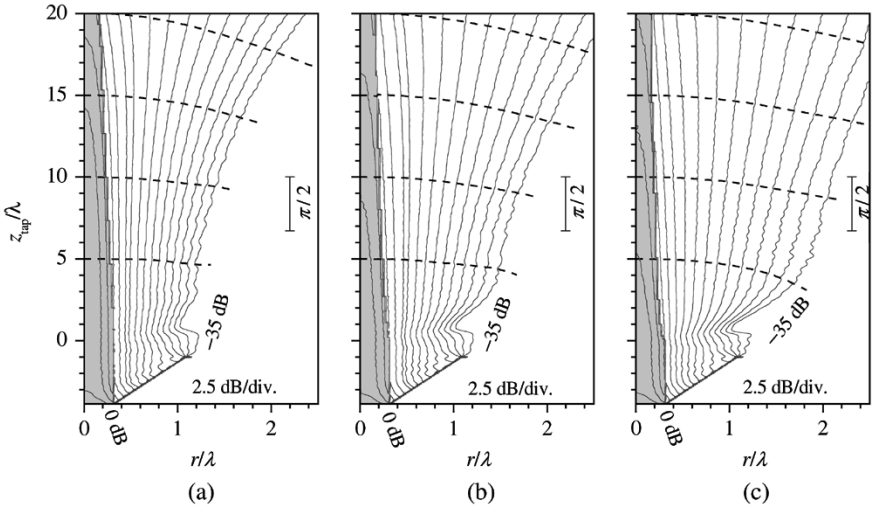

Fig. 7. Field distributions near tapered rods with $L_{\rm tap} = 20\lambda$ (half region); amplitude —, phase − − −. (a) Linear $(n = 1)$. (b) Curvilinear $(n = 2)$. (c) Curvilinear $(n = 3)$.

nearly agree with the theoretical results that assume no reflection at the free end.

B. Guided-Mode Conversion and Directivity

The gain of a dielectric rod increases with an expansion of the equiphase field region in the terminal aperture [13]. As is well-known, the field profile of the $\rm HE_{11}$ mode is extended into the air region by reducing the diameter of a rod [4]. Hence, the enhanced gain is obtained, if the $\rm HE_{11}$ mode excited at the feed end is smoothly converted into that at the free end where the diameter is reduced. To achieve smooth guided-mode conversion, we should gradually reduce the diameter in the forward direction. In this section, the effect of the guided-mode conversion on the directivity is investigated in detail.

The diameter of the tapered rod connected with the uniform rod $(L_{\rm uni} = \lambda)$ is reduced from $2\rho_{\rm feed} = 0.64\lambda$ to $2\rho_{\rm free} = \rho_{\rm feed} = 0.32\lambda$, in which the phase constant (k_z) of the $\rm HE_{11}$ mode wave at the free end is reasonably close to the free-space wave number (k_0) [10], i.e., $k_z/k_0 = 1.005$. The directivity depends on a taper profile [11], so that several profiles of tapered rods are investigated by changing the parameter n in (1).

Note that Ladouceur and Love [20] intuitively described a low-loss criterion for a taper profile of a dielectric-waveguide. Radiation loss will be small if the taper length is large compared with the coupling length between the fundamental guided-mode and the radiation field. The limit of the local taper angle $(\Omega(z_{\rm tap}))$ between the z axis and the tangent to the dielectric interface was expressed as

$$\Omega(z_{\rm tap}) = \tan^{-1}\frac{\rho(z_{\rm tap})[k_z(z_{\rm tap}) - k_0]}{2\pi} \simeq \frac{\rho(z_{\rm tap})[k_z(z_{\rm tap}) - k_0]}{2\pi} \quad (2)$$

where $k_z(z_{\rm tap})$ is the phase constant of the $\rm HE_{11}$ mode at $z_{\rm tap}$. This equation implies that the change in $\rho(z_{\rm tap})$ should become less for larger $z_{\rm tap}$. Therefore, the guided mode power is expected to be maintained in a curvilinear taper compared with a linear taper.

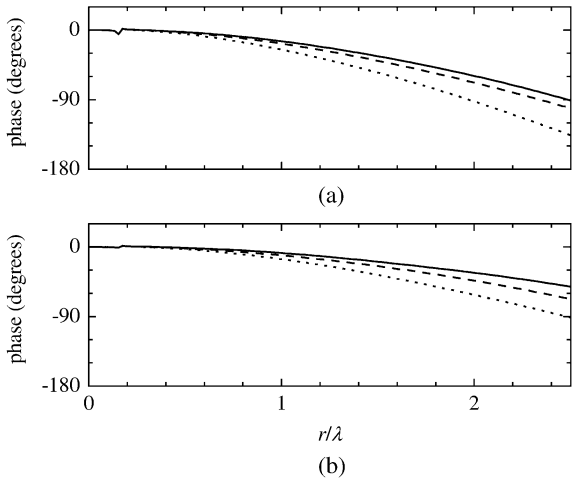

Fig. 8. Phase distributions at free ends (half region); linear $(n = 1)\cdots$, curvilinear $(n = 2)- - -$, curvilinear $(n = 3)$—. (a) $L_{\rm tap} = 10\lambda$. (b) $L_{\rm tap} = 20\lambda$.

Fig. 6 shows the guided mode power as a function of $z_{\rm tap}$ for $L_{\rm tap} = 10\lambda$ and 20λ, in which the overlap integral between the eigenmode field of the tapered rod and the numerically determined field is used, as in the case of Fig. 3. The power is normalized to the $\rm HE_{11}$ mode power excited at the feed end. It is found that the guided-mode power for the linear taper drastically decreases near the free end. On the other hand, the guided mode for the curvilinear taper can smoothly be converted with an increase in $L_{\rm tap}$, so that the considerable amount of the power is maintained at the free end. This tendency becomes more appreciable for a longer tapered rod. A value of 87% is obtained in a curvilinearly tapered rod of $n = 3$ with $L_{\rm tap} = 20\lambda$ (The reflected power generated in the tapered section is negligible and is calculated to be less than 0.05%). As a result, smooth guided-mode conversion can be achieved in a curvilinearly tapered rod, whose radius slightly varies near the free end.

Fig. 7(a)–(c) compare the field distributions along the tapered rods with $L_{\rm tap} = 20\lambda$. The solid lines present the amplitude of $|\rm E_r|$ and dashed lines present the phase at $z_{\rm tap} = 5\lambda, 10\lambda, 15\lambda,$

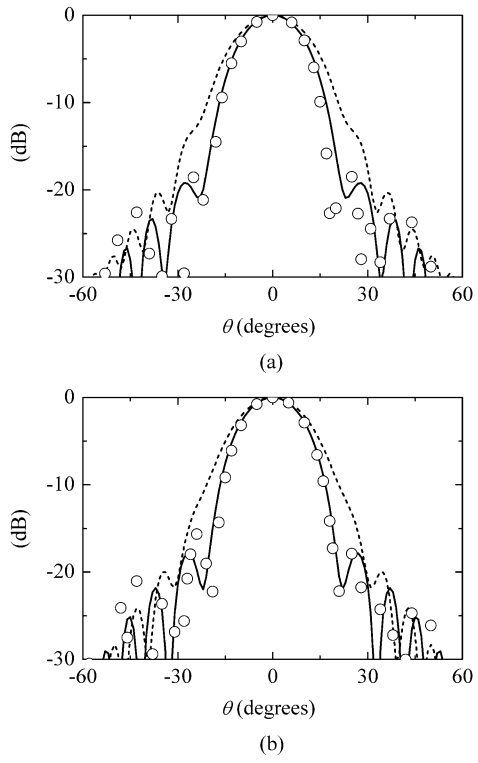

Fig. 9. Radiation patterns for $L_{\rm tap} = 10\lambda$; theoretical $(n = 1)\cdots$, theoretical $(n = 3)$—, experimental $(n = 3)$ ∘ ∘ ∘. (a) E-plane. (b) H-plane.

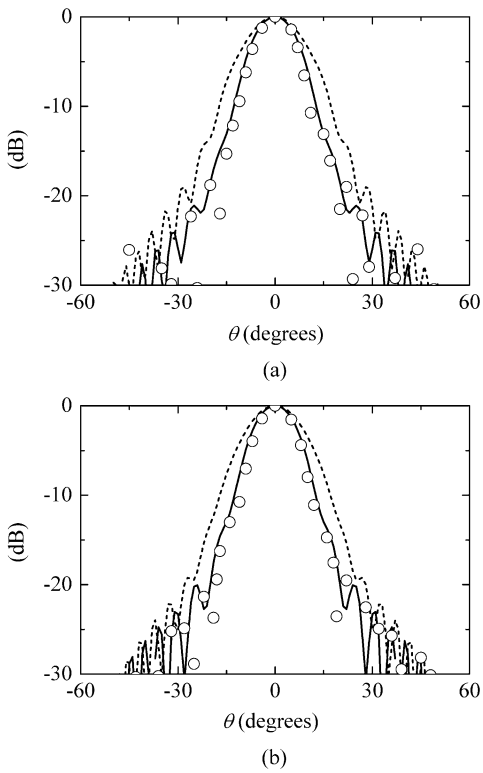

Fig. 10. Radiation patterns for $L_{\rm tap} = 20\lambda$; theoretical $(n = 1)\cdots$, theoretical $(n = 3)$—, experimental $(n = 3)$ ∘ ∘∘. (a) E-plane. (b) H-plane.

and 20λ. It is clearly observed that the fields along the curvilinearly tapered rods gradually extend into the air region near the free end in comparison to the field along the linearly tapered rod. The gradual extension of the field results in the expansion of the equiphase field region in the terminal aperture.

The phase distributions in the terminal apertures of tapered rods are plotted in Fig. 8(a) and (b): (a) is for $L_{\rm tap} = 10\lambda$ and (b) is for $L_{\rm tap} = 20\lambda$. It is found that the equiphase region is expanded, as n and $L_{\rm tap}$ are increased. The expansion of the equiphase region corresponds to an increase in the guided-mode power observed in Fig. 6. Owing to the expansion of the equiphase field region, a narrowed radiation pattern is expected.

Figs. 9 and 10 plot the typical radiation patterns for $L_{\rm tap} = 10\lambda$ and $L_{\rm tap} = 20\lambda$, respectively. The broken and solid lines present the theoretical results for the linearly $(n = 1)$ and curvilinearly $(n = 3)$ tapered rods, respectively. It can be said that the main beam becomes narrow as $L_{\rm tap}$ is lengthened from 10λ to 20λ. Furthermore, the pattern of the curvilinear taper has a sharper beam than that of the linear taper. The half-power beamwidth for $L_{\rm tap} = 20\lambda$ changes from $\pm 9.5^\circ$ to $\pm 7.5^\circ$ in the E- and H-planes, when n is increased from 1 to 3. The theoretical results agree well with the experimental results presented by open circles.

Fig. 11 plots the gain in the endfire direction $(\theta = 0)$ against $L_{\rm tap}$. As can be seen, the gain increases with an increase in $L_{\rm tap}$. The gain at $L_{\rm tap} = 20\lambda$ for $n = 3$ is calculated to be 22.2 dBi, which is a 2.5 dB increase compared with that for $n = 1$. Similar tendency is observed in the experimental results plotted by open squares and circles ($L_{\rm tap} = 0, 10\lambda$, and 20λ). Auxiliary calculations show that a gain of greater than 20 dBi is

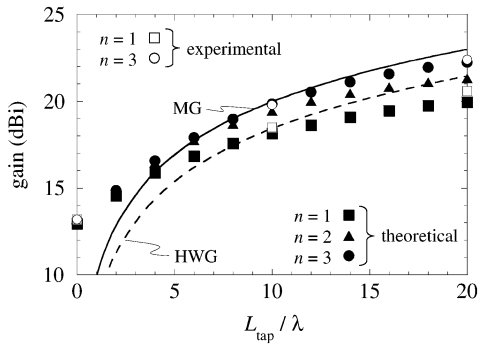

Fig. 11. Gain as a function of $L_{\rm tap}$.

maintained in a tapered rod of $n = 3$ with $L_{\rm tap} = 20\lambda$ over a frequency range of 10 to 12.7 GHz (24% bandwidth).

Finally, we compare the gain obtained from the FDTD analysis with that from the design guideline presented by Zucker [10]: The gain variation with $L_{\rm tap}$ is expressed as

$$G \cong m\frac{L_{\rm tap}}{\lambda} \tag{3}$$

where m is a variable. The data for $m = 7$ corresponds to the so-called Hansen–Woodyard gain (HWG), and that for $m = 10$ to the maximum gain (MG). The HWG and MG are plotted by dashed and solid lines in Fig. 11, respectively. It is found that a value of higher than the HWG can be obtained in a curvilinearly tapered rod of $n = 3$. On the other hand, the MG indicates that the gain of a rod with $L_{\rm tap} = 20\lambda$ is approximately 23 dBi. For reference, we further evaluate curvilinearly tapered rods for larger values of n using the BOR-FDTD method. Although not

presented, the gain reaches a value of 22.6 dBi when n is chosen to be 5, while a guided mode power of 82% is maintained at the free end. Consequently, the design guideline is effective in predicting the gain increase with an increase in L_{tap}, and roughly estimating the gain of a long tapered rod.

IV. Conclusion

We have numerically analyzed linearly and curvilinearly tapered cylindrical-dielectric-rods using the BOR-FDTD method, and investigated the effect of the guided-mode conversion in the rods on the directivity. Before evaluating the wave propagating along the tapered rod, we have designed a feeding system composed of a launching horn and a uniform rod whose feed end is tapered and inserted into the metallic waveguide, to efficiently excite the fundamental guided-mode of the uniform rod. After confirming the effectiveness of the feeding system, guided-mode conversion properties have been evaluated in the linearly and curvilinearly tapered rods. As a result, the fundamental guided-mode excited at the feed end is smoothly converted into that at the free end in the curvilinearly tapered rod. It is demonstrated that the smooth guided-mode conversion leads to the expansion of the equiphase field region in the terminal aperture with a subsequent increase in the gain. A gain of greater than 22 dBi can be obtained for the curvilinearly tapered rod with a length of 20λ. The calculated radiation patterns agree well with the experimental results.

References

[1] R. E. Collin and F. J. Zucker, *Antenna Theory*. New York: McGraw-Hill, 1969.

[2] E.-G. Neumann, "Radiation mechanism of dielectric-rod and Yagi aerials," *Inst. Elect. Eng. Electron. Lett.*, vol. 6, pp. 528–530, 1970.

[3] J. B. Andersen, *Metallic and Dielectric Antennas*. Lyngby, Denmark: Polyteknisk Forlag, 1971.

[4] A. D. Yaghjian and E. T. Kornhauser, "A modal analysis of the dielectric rod antenna excited by the HE_{11} mode," *IEEE Trans. Antennas Propag.*, vol. AP-20, no. 2, pp. 122–128, Mar. 1972.

[5] Y. Shiau, "Dielectric rod antennas for millimeter-wave integrated circuits," *IEEE Trans. Microw. Theory Tech.*, vol. MTT-24, no. 11, pp. 869–872, Nov. 1976.

[6] T. Takano and Y. Yamada, "The relation between the structure and the characteristics of a dielectric focused horn," *Trans. IECE*, vol. J60-B, no. 8, pp. 593–395, 1977.

[7] S. Kobayashi, R. Mittra, and R. Lampe, "Dielectric tapered rod antennas for millimeter-wave applications," *IEEE Trans. Antennas Propag.*, vol. AP-30, no. 1, pp. 54–58, Jan. 1982.

[8] R. Chatterjee, *Dielectric and Dielectric-Loaded Antennas*, London, U.K.: Research Studies Press, 1985.

[9] F. Schwering, A. A. Oliner, Y. T. Lo, and S. W. Lee, "Millimeter-wave antennas," in *Antenna Handbook*. New York: Van Nostrand Reinhold, 1993, vol. 3, ch. 17.

[10] F. J. Zucker and R. C. Johnson, "Surface-wave antennas and surface-wave excited arrays," in *Antenna Engineering Handbook*, 3rd ed. New York: McGraw-Hill, 1993, ch. 12.

[11] J. R. James, "Engineering approach to the design of tapered dielectric-rod and horn antennas," *The Radio and Electronic Eng.*, vol. 42, no. 6, pp. 251–259, 1972.

[12] T. Ando, J. Yamauchi, and H. Nakano, "Numerical analysis of a dielectric rod antenna—Demonstration of the discontinuity-radiation concept," *IEEE Trans. Antennas Propag.*, vol. 51, no. 8, pp. 2007–2013, Aug. 2003.

[13] ——, "Rectangular dielectric-rod fed by metallic waveguide," in *Proc. Inst. Elect. Eng. Microwave Antennas Propag.*, vol. 149, 2002, pp. 92–97.

[14] D. B. Davidson and R. W. Ziolkowski, "Body-of-revolution finite-difference time-domain modeling of space-time focusing by a three-dimensional lens," *J. Opt. Soc. Amer. A*, vol. 11, no. 4, pp. 1471–1490, 1994.

[15] A. Taflove and S. C. Hagness, *Computational Electrodynamics, The Finite-Difference Time-Domain Method*, 2nd ed. Boston, MA: Artech House, 2000.

[16] W. Yu, N. Farahat, and R. Mittra, "Far-field pattern calculation in body-of-revolution finite-difference time-domain (BOR-FDTD) method," *Microw. Opt. Tech. Lett.*, vol. 31, no. 1, pp. 47–50, 2001.

[17] T. Ando, S. Numata, J. Yamauchi, and H. Nakano, "Numerical analysis of a tapered dielectric-rod antenna using the body-of-revolution FDTD method," in *Asia Pacific Microwave Conf. Dig.*, vol. 3, 2002, pp. 1633–1636.

[18] C. A. Balanis, *Advanced Engineering Electromagnetics*. New York: Wiley, 1989.

[19] S. T. Chu, W. P. Huang, and S. K. Chaudhuri, "Simulation and analysis of waveguide based optical integrated circuits," *Computer Phys. Commun.*, vol. 68, pp. 451–484, 1991.

[20] F. Ladouceur and J. D. Love, *Silica-Based Buried Channel Waveguides and Devices*. London, U.K.: Chapman & Hall, 1996.

Takashi Ando (S'99–M'03) was born in Ibaraki, Japan, on March 14, 1969. He received the B.E., M.E., and Dr.E. degrees from Hosei University, Tokyo, Japan, in 1991, 1993, and 2003, respectively.

From 1993 to 1998, he was with TDK Corporation, Chiba, Japan. Since 2003, he has been with Hitachi Research Laboratory, Hitachi, Ltd., Ibaraki. His research interests include optical waveguides, dielectric antennas and nanotechnologies.

Dr. Ando is a Member of the Institute of Electronics, Information and Communication Engineers (IEICE) of Japan. He received an IEEE AP-S Japan Chapter Young Engineer Award, in 2002.

Isao Ohba was born in Osaka, Japan, on February 23, 1979. He received the B.E. and M.E. degrees from Hosei University, Tokyo, Japan, in 2002 and 2004, respectively.

He joined Toshiba Corporation, Tokyo, in 2004. His research interests include numerical analysis of dielectric waveguides.

Mr. Ohba is a Member of the Institute of Electronics, Information and Communication Engineers (IEICE) of Japan.

Satoshi Numata was born in Kanagawa, Japan, on May 27, 1977. He received the B.E. and M.E. degrees from Hosei University, Tokyo, Japan, in 2000 and 2002, respectively.

He joined Sony Corporation, Tokyo, Japan, in 2002.

Mr. Numata is a Member of the Institute of Electronics, Information and Communication Engineers (IEICE) of Japan.

Junji Yamauchi (M'85) was born in Nagoya, Japan, on August 23, 1953. He received the B.E., M.E., and Dr.E. degrees from Hosei University, Tokyo, Japan, in 1976, 1978, and 1982, respectively.

From 1984 to 1988, he served as a Lecturer in the Electrical Engineering Department of Tokyo Metropolitan Technical College. Since 1988, he has been a member of the faculty of Hosei University, where he is now a Professor of electronic informatics. His research interests include optical waveguides and circularly polarized antennas. He is the author of *Propagating Beam Analysis of Optical Waveguides* (U.K.: Research Studies Press, 2003).

Dr. Yamauchi is a Member of the Optical Society of America and the Institute of Electronics, Information and Communication Engineers of Japan.

Hisamatsu Nakano (M'75–SM'87–F'92) was born in Ibaraki, Japan, on April 13, 1945. He received the B.E., M.E., and Dr.E. degrees in electrical engineering from Hosei University, Tokyo, Japan, in 1968, 1970, and 1974, respectively.

Since 1973, he has been a member of the faculty of Hosei University, where he is now a Professor of electronic informatics. He was a Visiting Associate Professor at Syracuse University, Syracuse, NY, during May to September 1981, a Visiting Professor at University of Manitoba, Canada, during March to September 1986, and a Visiting Professor at the University of California, Los Angeles, during September 1986 to March 1987. He has published more than 190 refereed journal papers and 150 international symposium papers on antenna and relevant problems. He is the author of *Helical and Spiral Antennas* (New York: Research Studies Press/Wiley, 1987). He published the chapter *Antenna analysis using integral equations*, in *Analysis Methods of Electromagnetic Wave Problems* (Norwood, MA: Artech House, 1996, vol. 2). His research topics include numerical methods for antennas, electromagnetic wave scattering problems, and light wave problems.

Dr. Nakano received an International Scientific Exchange Award from the Natural Sciences and Engineering Research Council of Canada. In 1987, he received the Best Paper Award from the IEE 5th International Conference on Antennas and Propagation. In 1994, he received the IEEE AP-S Best Application Paper Award (H. A. Wheeler Award).